المجلة العراقية للبحوث الإنسانية والإجتماعية والعلمية
Iraqi Journal of Humanitarian, Social and Scientific Research
Print ISSN 2710-0952 Electronic ISSN 2790-1254
العـــدد 17 أيـار 2025
No.17 May 2025

Study of the effect of continuous laser (450nm) on the optical and structural properties of a thin film of organic semiconductor (TPD)

Noor Rabah Taha
Faleh Lafta Mater
Tikrit University - College of Science - Department of Physics
Faleh.l.mater@tu.edu.iq

Abstract

Because of their unique properties, Organic semiconductors are considered among the most promising materials in semiconductor applications. Before the irradiation process using laser, the optical properties of a samples of an organic semiconductor material (TPD) were prepared, examined and analyzed using (UV), (FTIR), and (XRD) devices. Then, the optical properties of the above-mentioned sample were again studied after irradiation for different durations utilizing a continuous semiconductor laser with output of (50000 mW) and a wavelength of (450 nm). The significance of this research concentrates on reduce the energy gap value of the organic compound after the irradiation. As a result, the organic compound will reduce the energy consumption required to facilitate the transfer of electrons from low to high levels, as well as the abundance of excited electrons between the two levels. This will lead to an increase in the number of photons emitted in this Kind of organic semiconductor material. This will facilitate the utilization of such organic materials in light-emitting diodes, which will serve as an alternative to conventional light-emitting diodes.

Keywords: Organic semiconductors material (TPD)**,** Inorganic semiconductors, Optical properties**,** Energy gap, laser treatment**.**

دراسة تأثير الليزر المستمر (450 نانومتر) على الخواص البصرية والبنيوية لغشاء رقيق من أشباه الموصلات العضوية(TPD)

نور رباح طه
فالح لفتة مطر
1، 2جامعة تكريت - كلية العلوم - قسم الفيزياء
Faleh.l.mater@tu.edu.iq

1.الملخص

نظرًا لخصائصها الفريدة، تعتبر أشباه الموصلات العضوية من بين أكثر المواد الواعدة في تطبيقات أشباه الموصلات. قبل عملية التشعيع باستخدام الليزر، تم تحضير الخواص البصرية لعينات من مادة أشباه الموصلات العضوية (TPD) وفحصها وتحليلها باستخدام أجهزة (UV) و (FTIR) و (XRD).ثم تمت دراسة الخواص البصرية للعينة المذكورة أعلاه مرة أخرى بعد التشعيع لفترات زمنية مختلفة باستخدام ليزر أشباه الموصلات المستمر بقوة خرج (50000 ميلي واط) وطول موجي (450 نانومتر). تتمحور أهمية هذا البحث حول تقليل قيمة فجوة الطاقة للمركب العضوي بعد التشعيع. ونتيجة لذلك، سيقلل المركب العضوي من استهلاك الطاقة المطلوبة لتسهيل نقل الإلكترونات من المستويات

المنخفضة إلى المستويات العالية، وكذلك وفرة الإلكترونات المثارة بين المستويين. سيؤدي هذا إلى زيادة عدد الفوتونات المنبعثة في هذا النوع من المواد شبه الموصلة العضوية. سيؤدي هذا إلى تسهيل استخدام مثل هذه المواد العضوية في الثنائيات الباعثة للضوء، والتي ستعمل كبديل للثنائيات الباعثة للضوء التقليدية.

الكلمات المفتاحية: مواد أشباه الموصلات العضوية (TPD)، أشباه الموصلات غير العضوية، الخصائص البصرية،

1. Introduction

Inorganic semiconductors such as silicon and germanium can be considered as the fundamental materials for the new electronic devices. Nevertheless, they have specific restrictions, such as the heaviness of weight for such materials in comparison with organic semiconductors, high manufacturing costs, and restricted flexibility. For this reason, exploring and developing organic semiconductors offers a possible option to overcome these obstacles, present a good method to solve these difficulties, and open the way for a new generation of electronics **[1]**. In recent years, organic semiconductors have experienced a quick growth as they have the ability to facilitate innovative electronic applications that exceed the possibilities of conventional crystalline inorganic semiconductors. The important distinctive properties of these materials render them considerable as a substitute for inorganic semiconductors **[2-5]**. Some of these properties of organic semiconductor materials are ease of manufacturing, ability to process at low temperatures, flexibility, ability to stretch and stretch, light weight, developed molecular structure control, low processes cost, the solution process ability, and the tuneable optoelectronic properties **[6-8]**. Furthermore, the other advantages include the ability for thin-film deposition on many different types of surfaces, mechanical flexibility, transparency, and the utilization of materials that are friendly to the environment. Applications include a range of both electronic and optoelectronic devices and systems **[9-10]**. The electronic configuration of such organic solar cells (OSCs) is essential for the maximum performance of thin-film devices. For example, between the lowest unoccupied molecular orbital (LUMO) and the highest occupied molecular orbital (HOMO), the variation in energy levels at the semiconductor heterojunction is a critical factor influencing the dissociation of photoexcited charges, as seen in organic photovoltaic devices (OPVs) **[11]**. Organic semiconductors (OS) possess numerous advantages over their counterparts of inorganic semiconductors. As a result, it can be used in a variety of applications, including biomedical sensors, image sensors, flexible microprocessors, photovoltaics, flexible displays, thin-film organic solar cells, OLED (Organic Light Emitting Diode) displays, OPV (Organic Photo-Voltaic) devices, and OFETs **[12-15]**.

2. Experimental Methods

N,N′ -Bis(3-methylphenyl)-N,N′ -diphenylbenzidine (TPD) is an organic powder with 99% purity and a chemical formula of $C_{38}H_{32}N_2$, its molecular weight is approximately 516.67 g/mol. It was obtained from Ossila Co. Photodetection applications utilize the TPD which is a p-type organic semiconductor with high hole mobility and excellent hole conduction. However, there are some parameters that impact the TPD hole transport properties like structure of the molecular, solid-phase packing arrangement, environmental stability, and energy reorganization during transfer of charges. Due to its significant emission at blue-violet range, TPD has been widely utilized in OLED manufacture and is a promising material for laser-active medium production **[16-20]**. The structure of molecular for TPD is shown in Fig. 1.

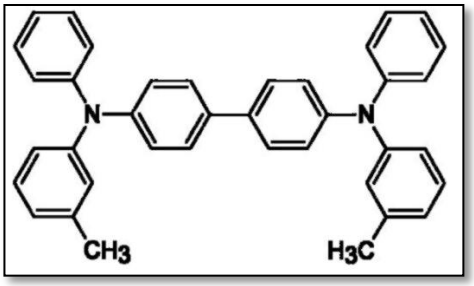

Figure 1. Chemical Structure of (TPD)

In this work, the spin casting technique was used to coat TPD organic material films onto the glass surface of substrates. The solution was prepared by dissolving TPD into Dichlorobenzene at a concentration of 50 mg/ml. A spin speed of 3000 rpm was then utilized to produce thin films. The prepared samples were irradiated using continuous semiconductor blue laser at a 450 nm wavelength in air. The laser beam diameter with 2mm and a max output of 50W was dispersed on the thin films surfaces using concave lens. The films were irradiated for different times Starting from 0, 10, 20, 30 and 40 minutes respectively. Optical properties such as absorption, reflection and transmissions spectra, , and of the main and irradiated samples of TPD films were studied utilizing spectrophotometer from the UV to the NIR band. To analyze the chemical composition and identify the presence of certain functional groups in the organic molecule thin film, FTIR was used to study the molecular fingerprint via the mechanism of chemical reactions spectrum of the molecule's absorption and transmission. Finally, XRD was used to study the crystalline structure of the samples before and after irradiation using laser.

5. Results and Discussion

5.1 Optical absorption and Optical absorption coefficient

The absorbance spectra of TPD thin films for the deposited and irradiated films for different times are shown in figure 2.

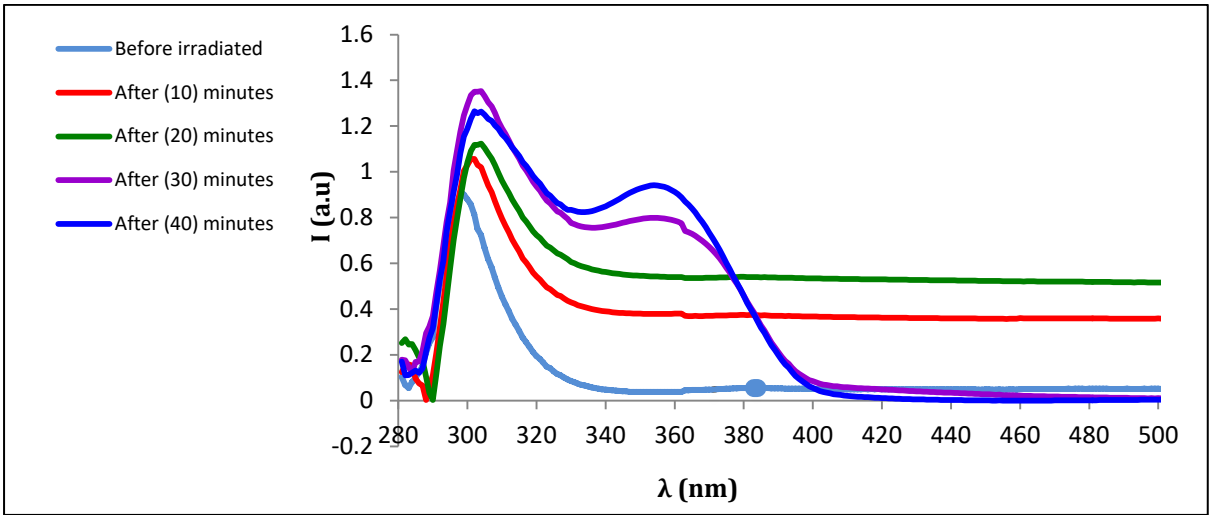

Figure 2. The absorbance spectra of TPD thin films for the deposited and irradiated films for different times

Here, a wide absorption band with a maximum wavelength of 300 nm and an intensity of 0.9 was examined. This transition appeared in the ultraviolet region as results of other electrons are being excited, which informs us about the electrical transition of molecules. Furthermore, compared to the film as deposited before irradiation, the absorption edge moves toward longer wavelengths (red shift). It can also be noted that the absorption intensity increases with increasing laser irradiation for different times, starting from (10, 20, 30 and 40 min) to reach the intensity of (1.05, 1.12, 1.4 and 1.26) respectively.

Therefore, the highest intensity ratio of (1.4) at (30 min) became the focus of interest and study in this research, as the irradiation duration increased, the intensity then decreased.

The absorption spectra of TPD thin film for the deposited and irradiated film for 30 minutes are shown in figure 3.

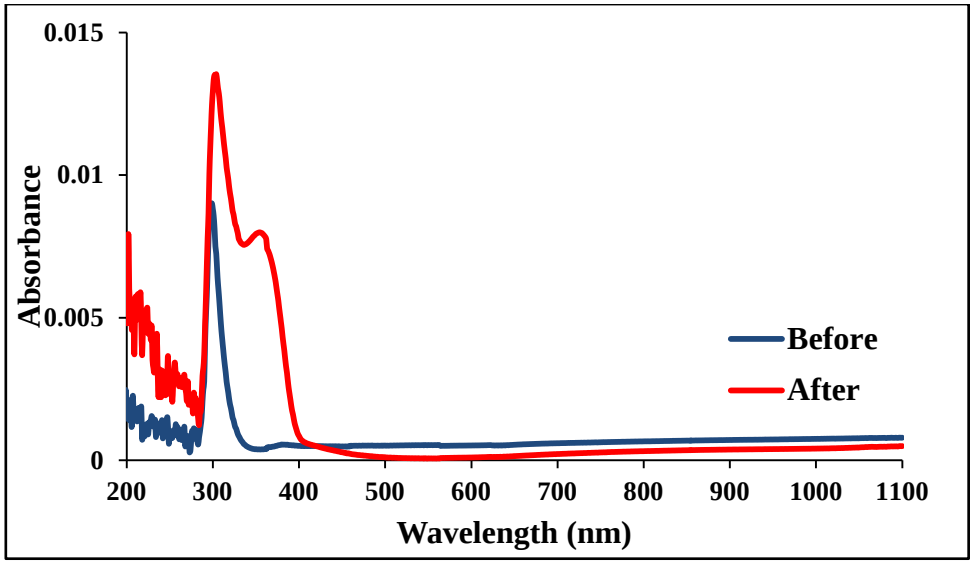

Figure 3. The absorbance spectra of TPD thin films for the deposited and irradiated films for 30 min

Figure 3 presents the absorption spectrum of pristine TPD thin film and for another TPD thin film exposed to laser irradiation for 30 minutes. Here, the absorption spectrum of TPD demonstrates a high increase in the ultraviolet region compared to the visible and near-infrared regions. It has a clear basic absorption edge close to 300 nm before irradiation and two another clear absorption peaks at 310 nm and 355 nm after irradiation. Due to transitions between the π-π* bond of biphenyl and π-π* bond of peripheral, two absorption peaks at 310 nm (4 eV) and 355 nm (3.49 eV) can be observed. This result is attributed to the HOMO band, which is spread in the carbon atoms between the biphenyl core and the peripheral ring, whereas the LUMO is mostly localised on the biphenyl centre.

Moreover, the absorption spectra peak could indicate to the peak of the surface Plasmon resonance peak. Such peaks may be caused by the collective oscillation of valence electrons that were excited using a laser beam, when the incident laser energy is corresponding to the surface electron oscillations natural frequency. The red shift in the peak of the absorption maximum happened because of the decrease in the energy gap. After laser treatment, the increase in the absorption spectrum of the irradiated samples is attributed to the dissociation of direct bonds within the molecular chains in the thin films of the organic material **[21]**. The optical absorption coefficients **[22]** of main and irradiated samples are determined from the transmittance data utilizing equation 1:

$$\alpha = \frac{1}{d}\ln\left[\frac{(1-R)^2}{2T} + \sqrt{\frac{(1-R)^4}{4T^2} + R^2}\right] \quad \text{..... (1)}$$

Here α , d , T and R are absorption coefficient , thickness of the thin films , transmittance and reflection respectively. The absorption coefficient of pristine TPD thin film and for another TPD thin film exposed to laser irradiation for 30 minutes is shown in Figure 4.

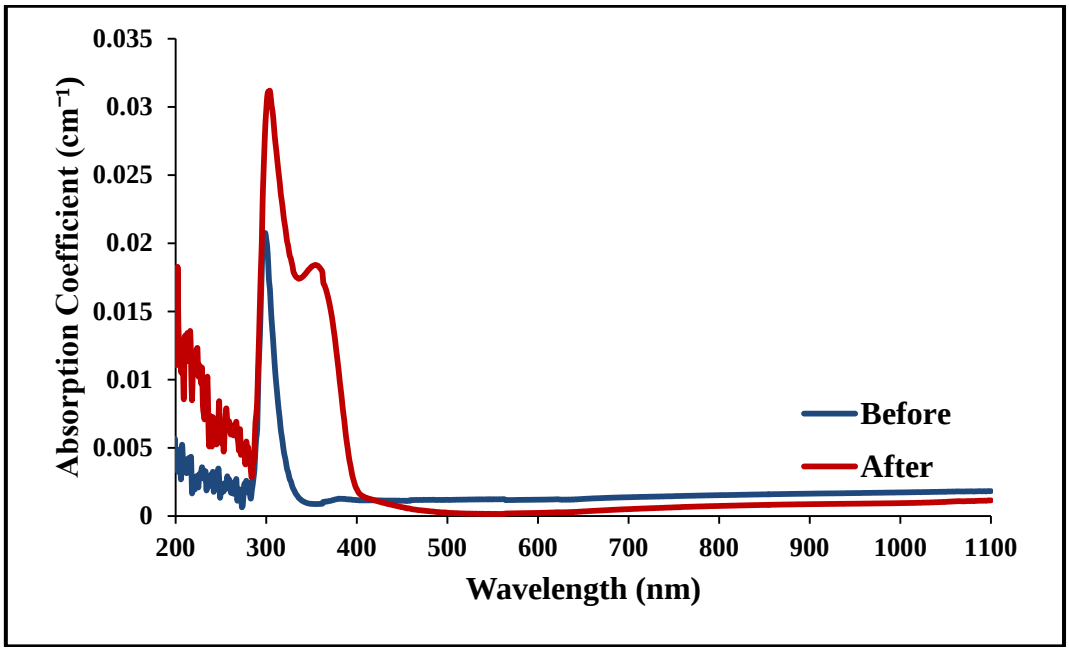

Figure 4. The absorption spectrum of pristine TPD thin film and for another TPD thin film exposed to laser irradiation for 30 minutes

After laser treatment, It is clear that the absorption coefficient of the samples increased. Such increasing in the absorption of irradiated sample in the ultraviolet wavelength is related to the carbon – oxygen bonds C–O and C=O. Such bonds reduced as a result to the laser treatment of the samples. The absorption coefficient (a) demonstrates how effectively the films can absorb light.

5.2 Transmittance and reflectance spectra

Transmittance T and reflectance R spectrum of TPD films are demonstrated in Figure 5. The variation in the roughness of the surface might explain the difference in the transmittance spectrum and reflectance spectrum seen after laser treatment. TPD transmittance is enormous in the range of $\lambda < 300$ nm. The high absorption of samples at the wavelength of 300 to 400 nm is related to the decrease in the energy gap. Then TPD transmittance increases noticeably in the range of $\lambda > 400$ nm, which may be attributed to the denaturation of TPD materials under laser treatment for 30 minutes [23].

.

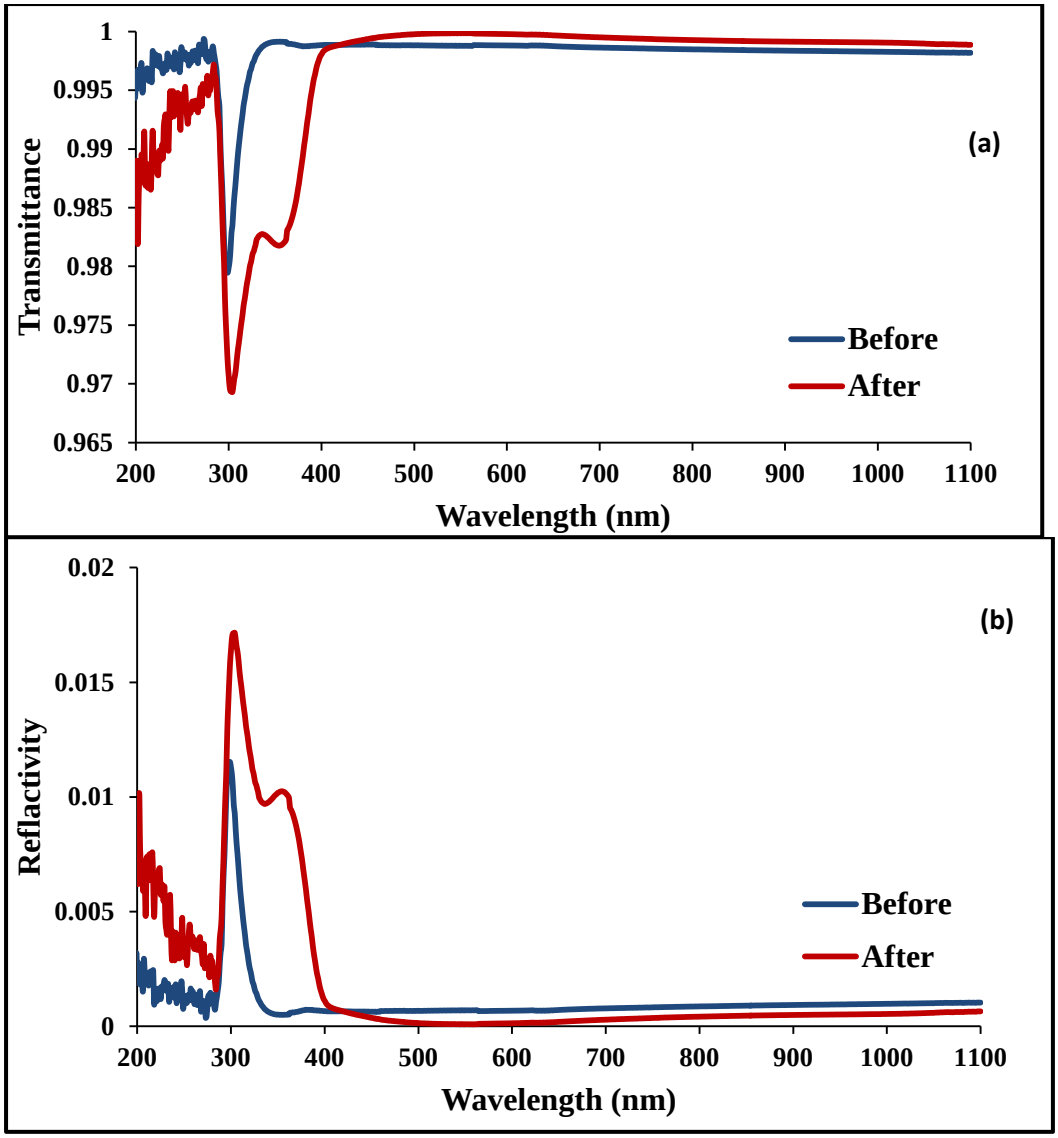

Figure 5. (a) The optical transmittance T and (b) reflectance R of TPD film and for another TPD thin exposed to laser irradiation for 30 minutes

5.3 Refractive index and extinction coefficient

The refractive index (n) and the extinction coefficient (k) data as functions of wavelength are illustrated in Figures 6 and 7.

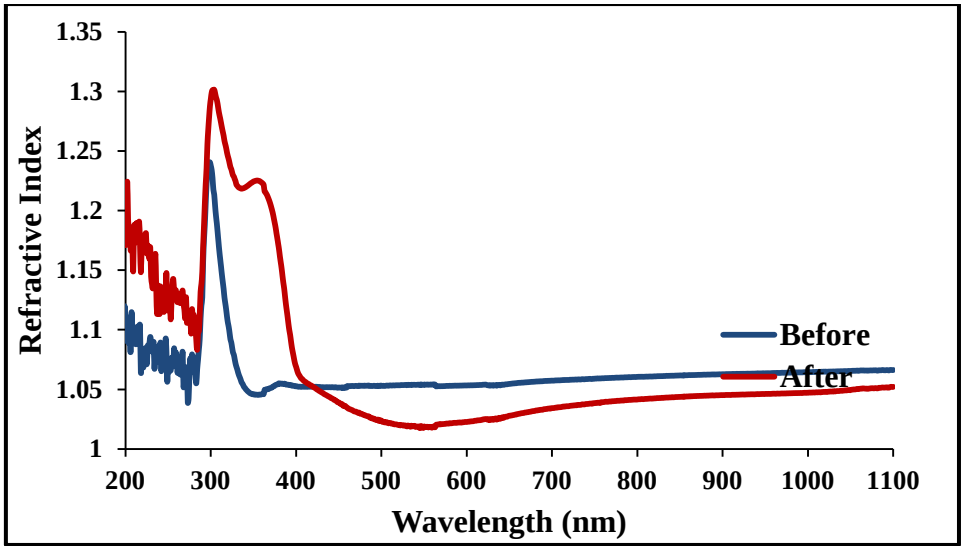

Figure 6. The refractive index (n) of TPD film and for another TPD thin exposed to laser irradiation for 30 minutes

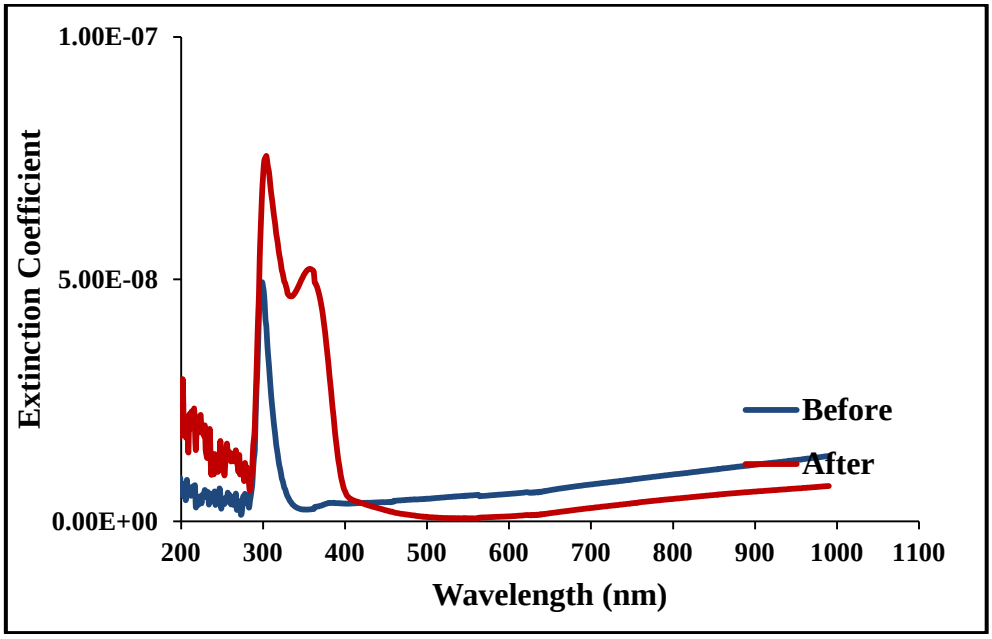

Figure 7. The extinction coefficient k of TPD film and for another TPD thin exposed to laser irradiation for 30 minutes

Calculation of the optical constants n and k when studying the optical properties of materials depends on equations 2:

$$n = \left(\frac{1+R}{1-R}\right) + \sqrt{\frac{4R}{(1-R)^2} - k^2} \quad \text{.....(2)}$$

in which $\boldsymbol{k = \frac{\alpha\lambda}{4\pi}}$

It can be seen that after laser treatment, the refractive index (n) and the extinction coefficient (k) increase are a result of the enhance in the absorption coefficient of treated samples. The increase in extinction coefficient can be attributed to microstructural defects. Ther defects inside the polymer lead to absorbing the dispersion of an incident photon resulting in the degradation of organic molecules for TPD. In addition, the diversity of the refractive index of TPD could be due to carbon bond polarization.

5.4 Dielectric properties

The dependencies of both imaginary and real parts on the photon wavelength of the samples are illustrated in Figures 8 and 9, respectively. Permittivity, or dielectric constant, is a fundamental dielectric characteristic that significantly influences material properties [24-25]. This is consequently associated with the dipole moment, molecule radius, specific and molar refraction, specific and molar dispersity, and dielectric susceptibility. The complex dielectric constant is described in equation 3:

$$\boldsymbol{\varepsilon = \varepsilon_r + i\varepsilon_i} \text{.....(3)}$$

The real part of the dielectric constant is (r), whereas the imaginary part is (i). For the dielectric constant, the real and imaginary components are shown in equations 4 and 5:

$$\boldsymbol{\varepsilon_r = n^2 - k^2} \text{ .....(4)}$$

and

$$\boldsymbol{\varepsilon_i = 2nk} \text{ .....(5)}$$

The dispersion is associated with the real part of the dielectric constant, whereas the dissipative rate of the wave in the medium is measured using the imaginary part.

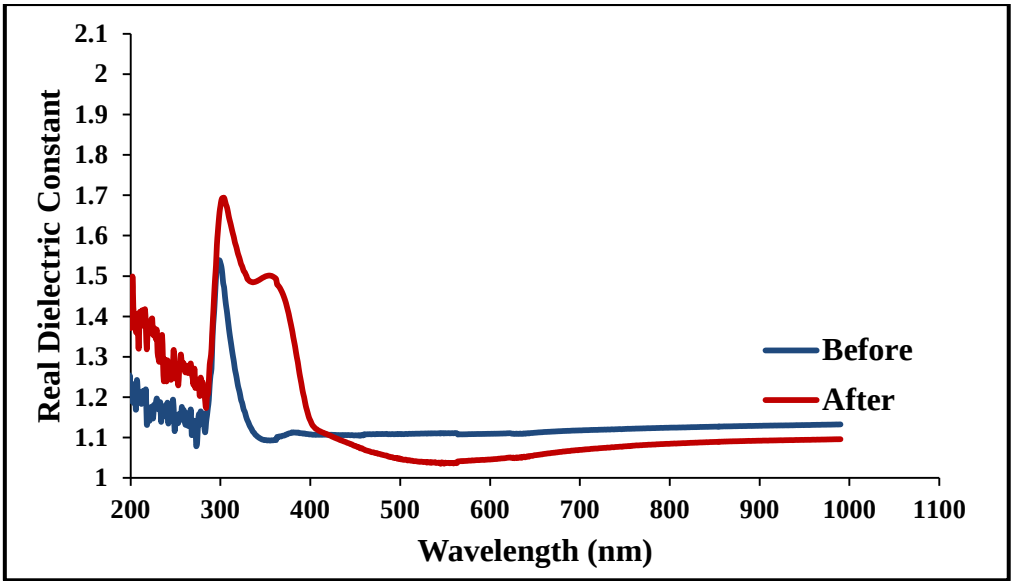

Figure 8. The real part of dielectric constant ε_r of TPD film and for another TPD thin exposed to laser irradiation for 30 minutes

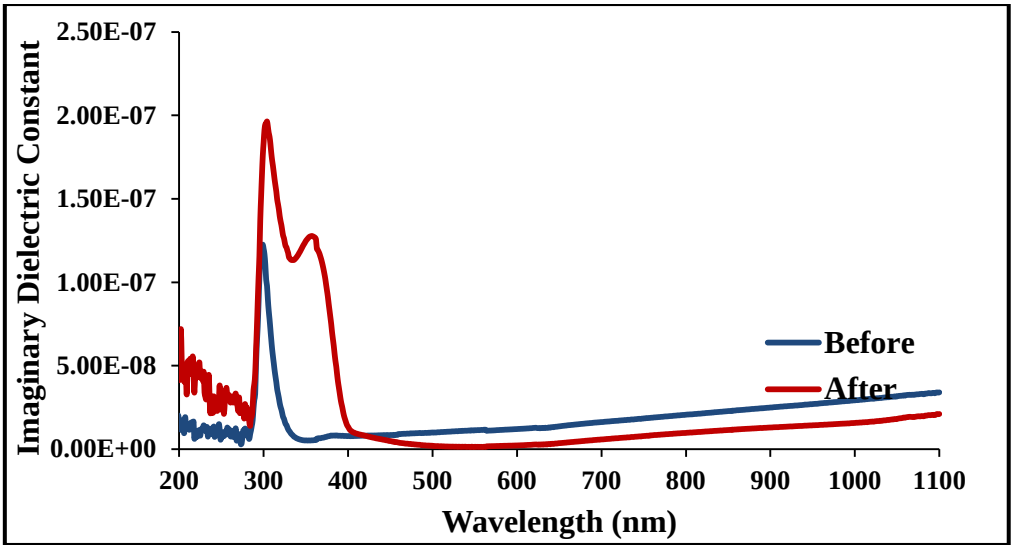

Figure 9. The imaginary part of dielectric constant of TPD film and for another TPD thin exposed to laser irradiation for 30 minutes

It can be seen that there is an increase in the real part of the dielectric constant ε_r with laser treatment as a result of normal dispersion in the TPD thin film. Moreover, it is concluded that the value of ε_r is larger than ε_i because (r) mainly depends on n^2. The peak appears in figure 8 and 9 shows the region of resonant absorption of the used TPD.

5.5 band gap energy

Figures 10 demonstrate the optical energy gap Eg of TPD films. Since it is so important for the design and development of such organic materials, the optical energy gap Eg is yet another crucial factor defining semiconductors and dielectric materials.

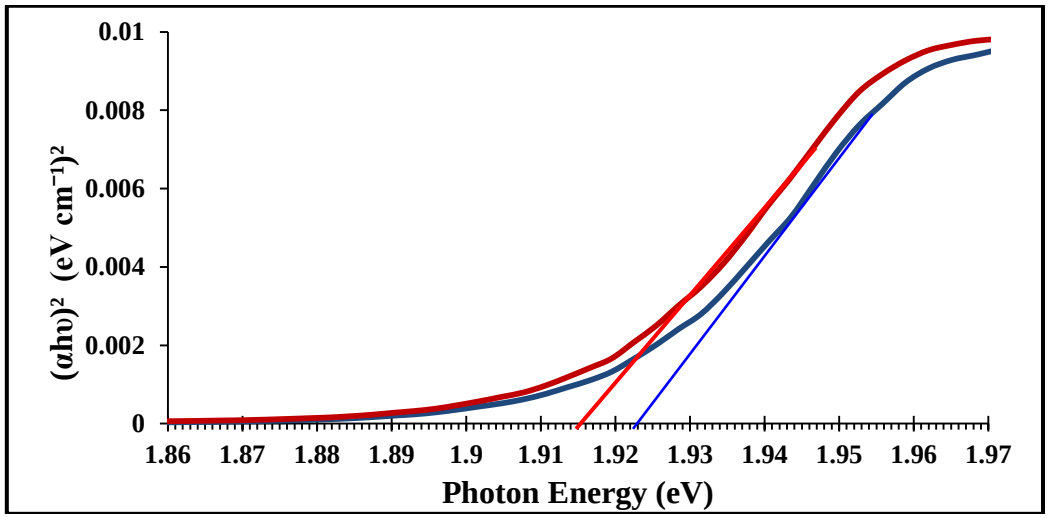

Figure 10. The energy gap of TPD film and for another TPD thin exposed to laser irradiation for 30 minutes

The intercept of the extrapolated linear part of the plot of $(\alpha h\sigma)^2$ with the photon energy was used to determine the optical energy gap of the samples. The samples' band gap energy dropped from 1.922 to 1.915 eV following laser treatment, as is clearly visible. One possible explanation is that the laser treatment increased the amount of C-H bonds and C=H groups in the samples. A wide variety of organic semiconductor applications rely on the bandgap as a critical criterion for material selection [26]. Interstitial states between the HOMO and LUMO bands, which minimise the energy gap, may be induced by certain structural defects and lattice disorders during laser irradiation.

5.6 Infrared spectroscopy (FTIR)

The FTIR method was utilized to investigate how laser irradiation effects the chemical structures of TPD thin films **[27]**. Figure 11 illustrates the infrared (IR) transmittance spectrum of TPD thin films before and after laser treatment for 30 minutes.

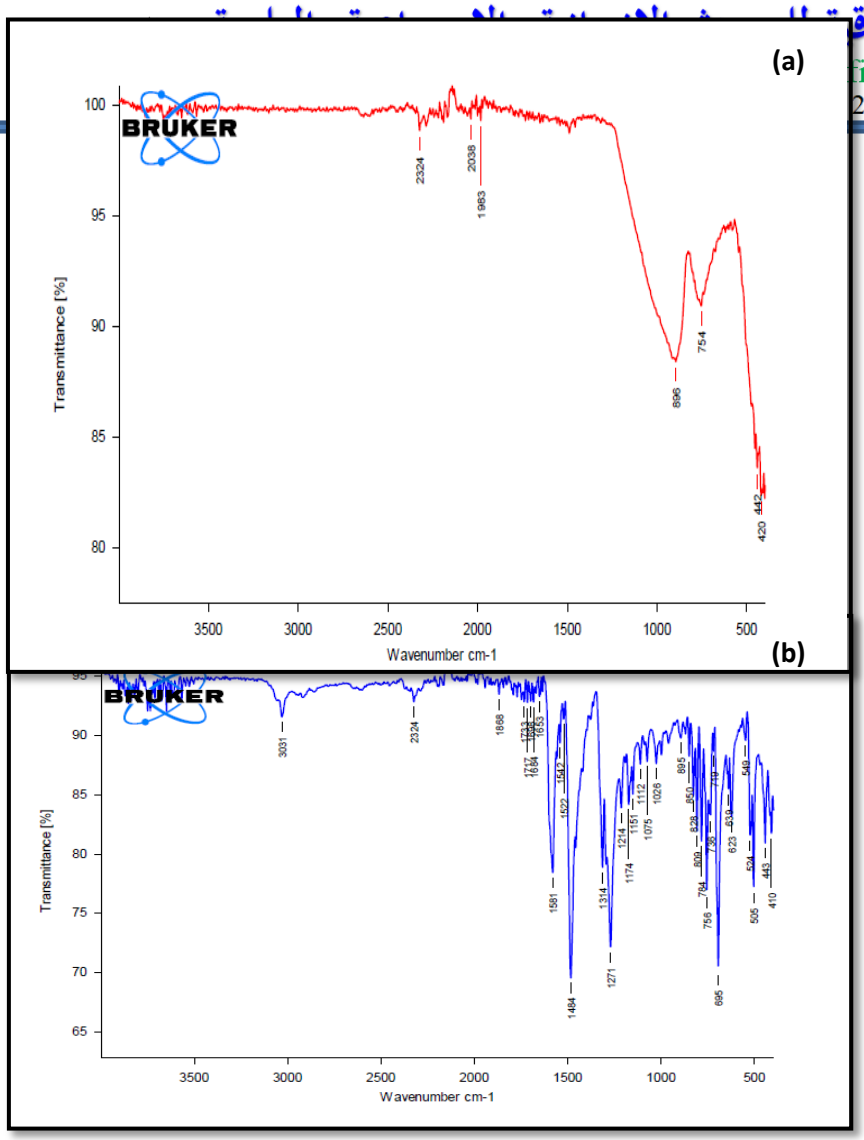

Figure 11. shows the IR transmittance spectra of TPD thin films, (a)before and (b) after laser treatment for 30 minutes.

It can be seen from figure 11(a) that the infrared spectra of TPD molecular bonds concentrate in six various regions around the wave numbers 420, 754, 896, 1983, 2038 and 2324 cm^{-1} before laser treatment. The infrared peaks in the spectral region (400-1500 cm^{-1}) consider as a fingerprint to pronounced –OH stretching peaks. However, after laser treatment, figure 11(b) shows the peak position of TPD thin film and fingerprint IR peaks in a wide range of spectral regions starting from 410 cm^{-1} to 3031 cm^{-1} may be ascribed to out of plane bending of C–H and stretching vibration of aromatic C–H overlapped with the vibrating of CH–C–CH, N–H and C–N respectively.

5.6 X-ray diffraction (XRD)

To determine the crystal structure and the chemical structure of TPD, which includes crystallite size, lattice constants or parameters, d spacing and FWHM, X-ray diffraction can be used. Characterization of TPD organic thin films can

be performed to identify properties including the composition, crystal structure and important information that is particularly valuable for assessing the intermolecular interactions between adjacent molecules **[28]**, where resultant intermolecular interactions involving π–π stacking strongly influence electronic behaviour **[29]**. From the XRD spectrum in Figure 12 of the TPD thin film before irradiation, it is clear that there are two diffraction peaks at 2θ = 9.71 and 25.06. Crystallite size can be calculated from high intensity full width at half maximum (FWHM) using the Scherrer equation **[30]**.

$$D = \frac{k\lambda}{B\cos\theta} \quad \text{.....(6)}$$

where D is the crystallite size, k is the shape factor of (0.9), λ is the X-ray wavelength of (0.154 nm), β is the full width at half maximum (FWHM) and θ is the Bragg angle. Such data for the calculation of crystallite size can be seen in Table 1.

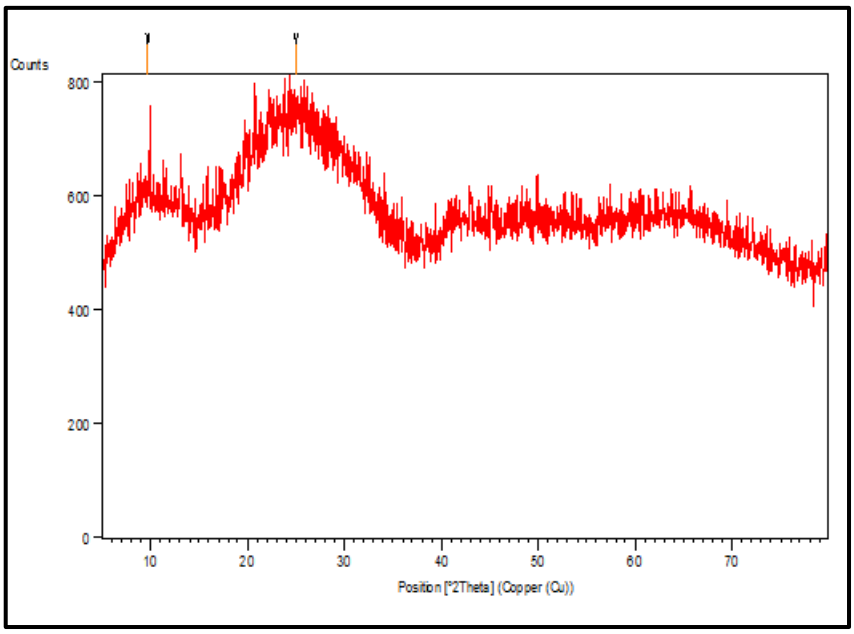

Figure 12. The Diffraction peaks for TPD film before laser treatment

Table 1: Structural parameters and Peak List of XRD results for TPD film before laser treatment

Pos.[°2Th.]	Height [cts]	FWHMLeft[°2Th.]	d-spacing [Å]	Rel. Int. [%]
9.716470	54.807510	4.636117	9.09545	24.07
25.016020	227.694100	9.097093	3.55671	100.00

From the XRD spectrum in Figure 13 of the TPD thin film after irradiation, it is clear that there are multi diffraction peaks at 2θ. Crystallite size can be

calculated from high intensity and full width at half maximum (FWHM) using the Scherrer equation at 2θ= 31.73 using table 2.

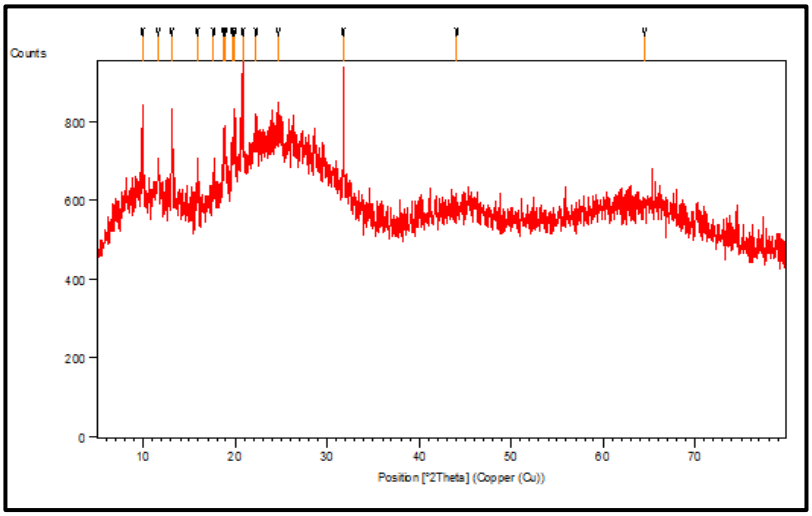

Figure 13. The Diffraction peaks for TPD film after laser treatment

Table 2: Structural parameters and Peak List of XRD results for TPD film after laser treatment

Pos.[°2Th.]	Height [cts]	FWHMLeft[°2Th.]	d-spacing [Å]	Rel. Int. [%]
9.895(7)	155(23)	0.12(3)	8.93204	65.61
11.59(3)	53(11)	0.25(4)	7.62831	22.55
13.103(6)	168(20)	0.12(2)	6.75145	70.93
15.84(1)	70(24)	0.13(8)	5.59167	29.51
17.65(2)	45(21)	0.12(7)	5.02185	19.11
18.73(2)	91(26)	0.13(5)	4.73274	38.71
18.92(1)	110(30)	0.11(5)	4.68763	46.47
19.65(2)	59(21)	0.15(6)	4.51446	24.87
19.93(1)	108(23)	0.16(5)	4.45063	45.77
20.788(9)	169(27)	0.16(5)	4.26949	71.46
22.25(4)	60(14)	0.4(2)	3.99295	25.43
24.7(1)	42(11)	1.3(4)	3.60867	17.95
31.739(6)	236(37)	0.09(2)	2.81702	100.00
44.1(3)	20(11)	5(2)	2.05243	8.37
64.5(2)	29(7)	7(1)	1.44419	12.42

From figures 12 and 13, it can be seen that from the XRD spectrum, a new diffraction peak was appeared. The appearance of the multi-peaks spectrum can be explained by the spatial fluctuation in density in the polymerized volume **[31]**. There is a peak shift observed in irradiated samples toward higher angles after laser treatment. It can be considered that the phase transformation led to both an overall decrease in the lattice constants as well as a contraction of the unit cells for these samples **[32]**. Moreover, the distance between planes of atoms (d-space)
that gives rise to diffraction peaks changed from 3.55671A^{o} before laser treatment to 2.81702A^{o} after laser treatment. The crystallite size was calculated using equation 6 to be 91 nm after laser treatment. The change in d-spacing and crystal size can be attributed to the incident energy, which can cause the direct bond breaking of molecular chains in the material, resulting in material removal by molecular fragmentation without significant thermal damage as a result of laser-materials interaction **[33]**.

Conclusions

In this work the influence of laser treatment on the optical properties and crystalline structure of TPD organic thin films was investigated. The absorption spectrum of irradiated samples increased after laser pulse treatment as a result of the direct bond breaking of molecular chains in the thin films of the organic material. Moreover, the value of the absorption coefficient was increased after laser pulse treatment. The band gap energy of the irradiated samples decreased with an increase of laser treatment duration. The impact of laser irradiation on refractive index and real – imaginary dielectric constant was also investigated. It can be observed that the real parts and imaginary parts increased. It can be attributed to the increase in the absorption coefficient. The FTIR technique shows multi- peak positions of TPD irradiated thin films and fingerprint IR peaks in a wide range of spectral regions which result from the bending of C–H and stretching vibrations of aromatic C–H overlapped with the vibrations of CH–C–CH, N–H and C–N respectively. Finally, the XRD spectrum shows multi-peaks spectrum in irradiated samples toward higher angles after laser treatment. It can be considered that the phase transformation leads to both an overall decrease in the lattice constants as well as a contraction of the unit cells for these samples.

References:

[1] Morab, S., Sundaram, M. M., & Pivrikas, A. (2023). Review on charge carrier transport in inorganic and organic semiconductors. Coatings, 13(9), 1657.

[2] Manikantan, N. A., & Sathya, P.(2024) Organic Semiconductors: Exploring Principles and Advancements in OPV and OLED-A International Journal of Electrical and Electronics Engineering, 11(5), 60-76.

[3] Diesing, S., Zhang, L., Zysman-Colman, E., & Samuel, I. D. W. (2024). A figure of merit for efficiency roll-off in TADF-based organic LEDs. Nature, 627(8005), 747-753.

[4] Stingelin, N., Jurchescu, O. D., Wakayama, Y., & Orgiu, E. (2023). Next-Generation Organic Semiconductors–Materials, Fundamentals, and Applications. Advanced Materials Interfaces, 10(19).

[5] Jin, H., Kim, K., Kim, K., Park, S., Shin, E. Y., Heo, J. W., ... & Son, H. J. (2024). Development of degradable networked-organic semiconductors and effects on charge carrier mobility in organic thin-film transistors. Journal of Materials Chemistry C.

[6] Kim, K., Yoo, H., & Lee, E. K. (2022). New opportunities for organic semiconducting polymers in biomedical applications. Polymers, 14(14), 2960.

[7] Chen, X., Wang, Z., Qi, J., Hu, Y., Huang, Y., Sun, S., ... & Hu, W. (2022). Balancing the film strain of organic semiconductors for ultrastable organic transistors with a five-year lifetime. Nature Communications, 13(1), 1480.

[8] Yumusak, C., Sariciftci, N. S., & Irimia-Vladu, M. (2020). Purity of organic semiconductors as a key factor for the performance of organic electronic devices. Materials Chemistry Frontiers, 4(12), 3678-3689.

[9] Sawatzki-Park, M., Wang, S. J., Kleemann, H., & Leo, K. (2023). Highly ordered small molecule organic semiconductor thin-films enabling complex, high-performance multi-junction devices. Chemical Reviews, 123(13), 8232-8250.

[10] Poriel, C., & Rault-Berthelot, J. (2023). Dihydroindenofluorenes as building units in organic semiconductors for organic electronics. Chemical Society

Reviews.

[11] Bertrandie, J., Han, J., De Castro, C. S., Yengel, E., Gorenflot, J., Anthopoulos, T., ... & Baran, D. (2022). The energy level conundrum of organic semiconductors in solar cells. Advanced Materials, 34(35), 2202575.

[12] Yang, X., & Ding, L. (2021). Organic semiconductors: commercialization and market. J. Semicond, 42(9), 090201.

[13] Pancaldi, A., Raimondo, L., Minotto, A., & Sassella, A. (2023). Post-growth dynamics and growth modeling of organic semiconductor thin films. Langmuir, 39(9), 3266-3272.

[14] Pope, T., Giret, Y., Fsadni, M., Docampo, P., Groves, C., & Penfold, T. J. (2023). Modelling the effect of dipole ordering on charge-carrier mobility in organic semiconductors. Organic Electronics, 115, 106760.

[15] Charoughchi, S., Liu, J. T., Berteau-Rainville, M., Hase, H., Askari, M. S., Bhagat, S., ... & Salzmann, I. (2023). Sterically-Hindered Molecular p-Dopants Promote Integer Charge Transfer in Organic Semiconductors. Angewandte Chemie, 135(31), e202304964.

[16] Holzer, W., Penzkofer, A., & Hörhold, H. H. (2000). Travelling-wave lasing of TPD solutions and neat films. Synthetic Metals, 113(3), 281-287.

[17] Gao, H. (2010). Theoretical characterization of hole mobility in N, N′-diphenyl-N, N′-bis (3-methylphenyl)-(1, 1′-biphenyl)-4, 4′-diamine. Journal of Molecular Structure: THEOCHEM, 962(1-3), 80-84.

[18] Arkan, E., Arkan, M. Z. Y., Unal, M., Yalcin, E., Aydin, H., Çelebi, C., ... & Demic, S. (2020). Performance enhancement of inverted perovskite solar cells through interface engineering by TPD based bidentate self-assembled monolayers. Optical Materials, 105, 109910.

[19] Paspirgelyte, R., Grazulevicius, J. V., Grigalevicius, S., & Jankauskas, V. (2009). N-(2, 2-Diphenylvinyl)-N, N′-diphenylbenzidine-based derivatives as hole-transporting glass-forming materials. Synthetic metals, 159(5-6), 487-491.

[20] Gao, H. (2010). Theoretical characterization of hole mobility in N, N′-diphenyl-N, N′-bis (3-methylphenyl)-(1, 1′-biphenyl)-4, 4′-diamine. Journal of Molecular Structure: THEOCHEM, 962(1-3), 80-84.

[21] Wangui, E., Ikua, B. W., & Nyakoe, G. N. (2022, June). A study on

influence of beam orientation in engraving using CO2 laser. In Proceedings of the Sustainable Research and Innovation Conference (pp. 126-131).

[22] Zahedi, S., & Dorranian, D. (2013). Effect of laser treatment on the optical properties of poly (methyl methacrylate) thin films. Optical review, 20, 36-40.

[23] Liu, J., Wang, C., Dang, Z., Chu, Y., & Zhang, Z. (2022). Thermally resettable laser transmission induced transparency in polymer waveguides at 635 nm. Optics Express, 30(10), 17529-17540.

[24] Torshkhoyeva, Z. S., Kunizhev, B. I., & Kharaev, A. M. (2023). The Investigation of the effect of laser radiation on the dielectric properties of polymethylmethacrylate. In E3S Web of Conferences (Vol. 413, p. 02039). EDP Sciences.

[25] Yang, X., Liu, J., & Koster, L. J. A. (2024). The Exceptionally High Dielectric Constant of Doped Organic Semiconductors. Advanced Electronic Materials, 2400413.

[26] Saqib, M., Rani, M., Mubashir, T., Tahir, M. H., Maryam, M., Mushtaq, A.,.. & Elansary, H. O. (2024). Designing of low band gap organic semiconductors through data mining from multiple databases and machine learning assisted property prediction. Optical Materials, 150, 115295.

[27] Khan, S. A., Khan, S. B., Khan, L. U., Farooq, A., Akhtar, K., & Asiri, A. M. (2018). Fourier transform infrared spectroscopy: fundamentals and application in functional groups and nanomaterials characterization. Handbook of materials characterization, 317-344.

[28] Schweicher, G., Das, S., Resel, R., & Geerts, Y. (2024). On the importance of crystal structures for organic thin film transistors. Crystal Structure Communications, 80(10).

[29] McHugh, C. J. (2024). Crystal clear: the impact of crystal structure in the development of high-performance organic semiconductors. Crystal Structure Communications, 80(11), 696-697.

[30] Astuti, B., Zhafirah, A., Carieta, V. A., Hamid, N., Marwoto, P., Nurbaiti, U., ... & Aryanto, D. (2020, June). X-ray diffraction studies of ZnO: Cu thin films prepared using sol-gel method. In Journal of Physics: Conference Series (Vol. 1567, No. 2, p. 022004). IOP Publishing.

[31] Klein, S., Crégut, O., Gindre, D., Boeglin, A., & Dorkenoo, K. D. (2005). Random laser action in organic film during the photopolymerization process. Optics Express, 13(14), 5387-5392.

[32] Mostafa, M., Ebnalwaled, K., Saied, H. A., Roshdy, R., Mostafa, M., Ebnalwaled, K., ... & Roshdy, R. (2018). Effect of laser beam on structural, optical, and electrical properties of BaTiO 3 nanoparticles during sol-gel preparation. Journal of the Korean Ceramic Society, 55(6), 581-589.

[33] Wangui, E., Ikua, B. W., & Nyakoe, G. N. (2022, June). A study on influence of beam orientation in engraving using CO2 laser. In Proceedings of the Sustainable Research and Innovation Conference (pp. 126-131).